Cancer Epidemiology 67 (2020) 101732

Contents lists available at ScienceDirect

Cancer Epidemiology

journal homepage: www.elsevier.com/locate/canep

CT scans in childhood predict subsequent brain cancer: Finite mixture modelling can help separate reverse causation scans from those that may be causal

Nicolas R. Smoll, John D. Mathews*, Katrina J. Scurrah

Melbourne School of Population and Global Health, University of Melbourne, 207 Bouverie Street Carlton, VIC, 3053, Australia

ARTICLE INFO

Keywords:
Finite mixture model
Latent class analysis
Machine learning
Radiation epidemiology
Brain cancer

ABSTRACT

Background: Excess brain cancers observed after computed tomography (CT) scans could be caused by ionizing radiation. However, as scans are often used to investigate symptoms of brain cancer, excess cancers could also be due to reverse causation bias. We used finite mixture models (FMM) to differentiate CT exposures that are plausibly causal from those due to reverse causation.

Methods: Persons with at least one CT scan exposure and a subsequent diagnosis of brain cancer were selected from a cohort of 11 million young Australians. We fitted FMMs and used the posterior probability to inform the choice of exclusion periods. We validated our findings using a separate clinical dataset describing the time between first symptoms and brain cancer diagnosis (pre-diagnostic symptomatic interval; PSI).

Results: The cohort included 1028 persons with a diagnosed brain tumor and exposed to a total of 1,450 CT scans. The best-fitting model was a generalized linear mixture model using the exponential distribution with three latent classes and two covariates (age at exposure and year of exposure). The 99th percentile classifier cutoff was 18.9 months. The sample-size weighted mean of the 99th percentile of the PSI, derived from clinical data, was 15.6 months.

Conclusions: To minimize reverse causation bias in studies of CT scan and brain cancer, the optimal exclusion period is one to two years (depending on the choice of classifier). This information will inform the interpretation of current and future studies.

1. Introduction

Ionizing radiation is a well-recognized carcinogen, but uncertainty remains about its effects in the low-dose range. [1] Some experts accept that there is no threshold dose below which radiogenic cancer cannot occur [2,3], although this is disputed by others [4,5]. Recently, follow-up studies of large populations exposed to computed tomography (CT) scans in childhood or adolescence have shown increased rates of leukemia, brain cancer, and most other cancers [6–10]. However, as CT scans undertaken shortly before cancer diagnosis are often part of that diagnostic process, such CT scans (in general terms, "reverse causation scans") may bias risk estimates, especially at short intervals after CT exposures. This has raised questions about how much of the association of CT scan radiation with brain cancer is attributable to reverse causation [11].

Assessing the effects of reverse causation in epidemiological studies is difficult. In large CT scan cohorts it is unusual to have detailed information on the reason or indication for performing the CT scan, making it difficult to separate scans that are plausibly causal from those that are due to reverse causation. Another approach is to use exclusion periods or exposure lagging to explore the likely impact of reverse causation. For example, an exclusion period of one year, would delete all exposures that occurred in the year before the diagnosis of brain cancer. For exposure lagging of one year, the CT scan exposure date is lagged by one year. Unfortunately, there is little evidence to support the choice of an exclusion or lag period, and current practice uses arbitrarily chosen periods. In this paper we use data from the Australian CT scan cohort to define an evidence-based exclusion period or lag period, and we compare this with the results of a literature review of relevant clinical data-sets. Although our analyses are of some relevance to the related topic of cancer latency, a detailed analysis of latency is beyond the scope of this paper.

* Corresponding author.
E-mail address: mathewsj@unimelb.edu.au (J.D. Mathews).

https://doi.org/10.1016/j.canep.2020.101732
Received 5 December 2019; Received in revised form 2 March 2020; Accepted 16 April 2020

2. Methods

Our study used data from the Australian cohort of 11 million young Australians aged 0–19 years and registered with Medicare (Australia's universal healthcare system); details of study design have been previously reported [8]. Briefly, the Australian Institute of Health and Welfare linked records of all individual Medicare-funded services, including CT scans, to any national cancer registrations for individuals in the cohort; de-identified but linked records were accessed for the current research. We selected persons from the cohort with a record of at least one CT scan exposure between 1985 and 2005 who also hada subsequent diagnosis of brain cancer between 1985 and 2012. Brain cancers included in this study were high and low-grade gliomas (ICD-O-3 codes 9380, 9440-9444, 9381-9384, 9400-9401, 9410-9411, 9420-9421, 9423-9424, 9430, 9450-9451, 9460), medulloblastomas, primitive neurectodermal tumors, ependymomas and chordomas (9372, 9390-9395). Clinical indication for individual CT scans are not included in Medicare records.

Exposure was defined as a CT scan before the age of 20 years. The interval period (L) is the time between the date of a CT scan exposure (j) and the date of any subsequent diagnosis of first cancer (t):

$$L = t - j$$

In Australia, t is usually the date of the pathology report that first confirmed the diagnosis of cancer [12].

2.1. Mixture model

Finite mixture models (FMMs) are used to model the probability of an observation belonging to a particular group (determined by categories of an unobserved variable) termed a *latent class*. In this application we seek to define the latent class of CT scans that are due to reverse causation (and its complement, the latent class of CT scans that are plausibly causal). We assumed a priori that the distribution of the interval period between exposure and cancer diagnosis was an additive sum of the two distributions: 1) reverse causation exposures (CT scans to diagnose underlying cancer) and 2) potentially causal exposures (CT scans for unrelated indications). We used an FMM and latent class analysis, implemented in Stata 16.0 (College Station, Texas), to classify CT scans based on the interval time L between CT scan and brain cancer diagnosis. The posterior probability of being in each class was then used to inform the choice of exclusion periods.

We fitted a generalized linear model with an exponential distribution for the interval times. We tested models with no covariates, with age at exposure as a binary variable created using the median age at exposure ($\leq$12.5 and $>$ 12.5 years), and with year of CT scan as a binary variable created using the median year of exposure ($\leq$1993 and $>$ 1993). Class enumeration was performed by selecting the model with the lowest Bayesian Information Criterion (BIC), as the final model [13]. A sensitivity analysis was then performed to assess the robustness of the model. The sensitivity analysis tested 1–4 classes, different combinations of covariates, and various combinations of normal, log-normal, Weibull, and exponential models. For example, a Weibull model for the reverse causation class with an exponential model for the causal class. Models were also fitted to various subsets of the data, namely CT scans of the brain, and excluding extremity scans only in sensitivity analyses.

2.2. Classifier

There are two methods of choosing a classifier used here. The crossover method uses an interval time cutoff at which the posterior probability of being classified in the late class is greater than the posterior probability of being classified in the earlier, or reverse causation class [14]. The 99th percentile method (a more conservative approach trialled here) uses an interval time cutoff at which the posterior probability of being classified in the late class is greater than the 99th percentile.

2.3. External validation using published clinical data

A narrative review of the literature based on a systematic search was performed to create a clinical dataset describing the pre-diagnostic symptomatic interval (i.e. the time from first symptom to diagnosis; PSI).

We reviewed reports of the PSI for brain cancer using the EMBASE and Medline search engines to measure the median PSI. We included articles published in both French (1 article) and English, and the search terms included "diagnosis AND delay AND tumor(s)" or "tumours", and "pre-diagnostic symptomatic interval", similar to the strategy used by Wilne et al. [15]. While not using the term "cancer" may have led to missed articles, we found enough articles for our purposes. Reference lists were searched for any missed studies. We searched articles published from January 2007 to December 2015, as Wilne et al. 2007 performed a comprehensive systematic review of the literature from previous years, finding a median pre-diagnostic symptomatic interval ranging from 1 to 27 months, with the longest median symptomatic interval occurring with biologically slow-growing tumors such as gangliogliomas [15].

Our inclusion criteria were articles reporting primarily on children and adolescents of less than 20 years of age and reporting on the PSI for primary brain cancers. We excluded articles that did not report a mean or median of the pre-diagnostic symptomatic interval. Articles reporting only on tumors of the head and neck (e.g., jaw, ear, eyes, nose) or tumors of the cranial nerves (e.g., optic nerve or schwannomas) and spine were also excluded.

2.4. Calculating percentiles of the PSI

The first step was to find the best-fitting underlying distribution of PSI values. Only two studies [16,17] presented this data as a histogram, allowing data extraction using WebPlotDigitizer [18]. We modelled the data from these two studies using non-linear regression to find the best-fitting probability distribution, using linear, logarithmic, inverse, quadratic, cubic, power, and exponential curves. Once the distribution was chosen, it could be used to calculate the cumulative density function and from this, percentiles. We chose the distribution with the best visual fit that resulted in the highest r-squared values. In our dataset, an underlying exponential distribution was found to be the best-fitting underlying distribution.

The median (or the mean if the median was not reported) was used to calculate the 99th percentile of the exponential distribution and its cumulative distribution function. The cumulative distribution function of the exponential distribution with a rate of λ and for values of x greater than or equal to zero is

$$F(x;\lambda) = 1 - e^{-\lambda x} \quad (1)$$

The rate parameter λ of the exponential distribution is calculated from the mean (μ) and median ($\mu^{1/2}$) using the following equations (median or mean PSI in weeks is typically used here):

$$\lambda = \frac{1}{\mu} \quad (2)$$

$$\lambda = \frac{\ln(2)}{\mu^{1/2}} \quad (3)$$

Using the estimate of the exponential distribution's rate parameter, we calculate the 75th (Eq. 4; P_{75}), 95th (Eq. 5; P_{95}), and 99th percentiles (Eq. 6; P_{99}).

$$P_{75} = \frac{-\log(0.25)}{\lambda} \quad (4)$$

$$P_{95} = \frac{-\log(0.05)}{\lambda} \quad (5)$$

$$P_{99} = \frac{-\log(0.01)}{\lambda} \quad (6)$$

To summarize the data, a sample-size weighted mean of the P_{75}, P_{95}, and P_{99} was calculated. This information was used to validate the choice of classifier (i.e. crossover vs 99th percentile).

With this new external clinical dataset, we modelled the 99th percentile of the PSI and compare this to the results of the FMM model to assess clinical validity. A CT scan occurring before the onset of the earliest symptoms or signs is unlikely to represent a CT scan associated with the diagnostic workup. Thus, the distribution of the PSI can validate the choice of FMM model classifier. We classify scans with an interval time greater than the 99th percentile of the PSI (P99) as potentially causal.

3. Results

The Australian Medicare cohort comprised 11,528,078 persons, of whom 1,028 had a CT scan before the age of 20 and before the diagnosis of a brain tumor. The average age at diagnosis was 14 years with an interquartile range (IQR) of 11. The range was 2 months to 46 years of age at diagnosis. Overall, 274 brain cancers were diagnosed after the age of 19. In those diagnosed before the age of 20 the median age was 11 (IQR 9). Of the 1,028 tumors, 605 were low and high-grade gliomas, 158 were medulloblastomas and primitive neurectodermal tumors and the rest consisted of ependymomas, chordomas and neuroblastomas. Meningiomas or CNS lymphomas were not included. In total there were 1,450 CT scans, of which 1,255 (87%) were CT scans of the brain. Of all scans, 65% occurred within one year, and 62% within six months, before a diagnosis of brain cancer. The median interval period for all CT scans was 4.7 weeks. The median interval period for CT scans of the brain was 3.3 weeks.

3.1. Model fitting

A generalized linear mixture model using the exponential distribution with three latent classes and age at exposure and year of exposure (dichotomized) as covariates was chosen as the best-fitting model because it had the lowest BIC (BIC = 2,048; see Table 1). This model initially showed three underlying distributions (shown in Fig. 1), the first two of which were collapsed into one (see below), representing the reverse causation class. When modelled separately, the younger populations had three classes while the older age groups had two classes (data not shown).

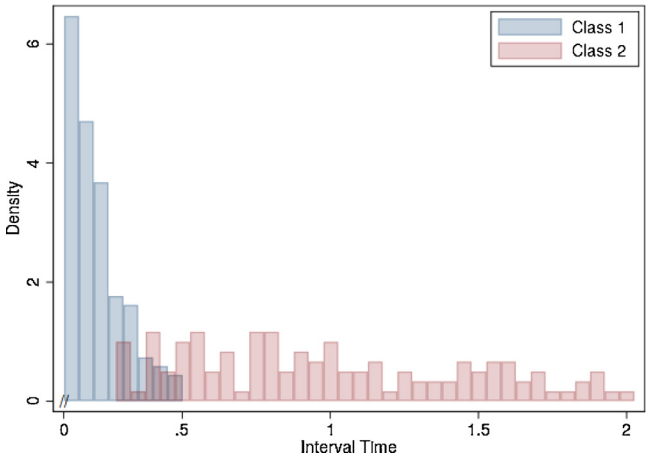

Fig. 1. Histogram of CT scan interval time (years) densities by class after classification. Class 1 (reverse causation class) were CT scans with a posterior probability greater than 50% of being in class 1 (uses crossover classification method). The final accepted model had three latent classes and two covariates (age at exposure, year of CT scan), but classes were collapsed to two classes. The first 5 weeks of scans are not included due to the large density of scans during this time.

We cannot confirm what each of the three classes represents in the younger group, but we believe the first class may represent mostly urgent care scans (likely including diagnostic CT scans), the second class may represent elective scans (including watch-and-wait CT scans [19]), and the third class, unrelated scans. For the younger population, we grouped the first two classes as one when describing the posterior probabilities as these two classes were CT scans occurring in those expected of having a brain cancer.

3.2. Means, medians, and upper 99th percentile

Table 2 reports the predicted mean, median, and upper 99th percentile of the interval period for each class. The mean, median, and upper 99th percentile of the interval period for the first class was 1.6, 1.0, and 7.8 weeks, respectively. The mean, median, and upper 99th percentile of the interval period for the second class was 10.4, 7.3, and 47.3 weeks, respectively. The mean, median, and upper 99th percentile of the interval period for third class was 9.7, 6.7, and 44.6 years,

Table 1
Comparison of models. The proportion (and 95% CI) of CT scans in each latent class is reported/shown. The basic model had no covariates. Models with one class were those assuming no unobserved groups and were the worst-fitting models. The best-fitting model (lowest BIC) was the model with three classes with two covariates.

Model	Class	BIC	Class 1 proportion	Class 2 proportion	Class 3 proportion	Class 4 proportion
No covariates	1	6329	1 (1,1)	–	–	–
No covariates	2	2143	0.57 (0.55,0.6)	0.43 (0.4,0.45)	–	–
No covariates	3	2096	0.49 (0.45,0.54)	0.12 (0.09,0.16)	0.39 (0.36,0.42)	–
No covariates	4	2110	0.17 (0,1)	0.32 (0,1)	0.12 (0.09,0.16)	0.39 (0.36,0.42)
Age at Exposure Only	1	6230	1 (1,1)	–	–	–
Age at Exposure Only	2	2114	0.57 (0.55,0.6)	0.43 (0.4,0.45)	–	–
Age at Exposure Only	3	2108	0.5 (0.45,0.55)	0.09 (0.05,0.15)	0.41 (0.38,0.43)	–
Age at Exposure Only	4	2129	0.5 (0.45,0.55)	0.09 (0.05,0.15)	0 (0,1)	0.41 (0.38,0.43)
Year of CT	1	6188	1 (1,1)	–	–	–
Year of CT	2	2116	0.43 (0.41,0.46)	0.57 (0.54,0.6)	–	–
Year of CT	3	2137	0.43 (0.41,0.46)	0 (0,1)	0.57 (0.54,0.6)	–
Year of CT	4	2112	0.39 (0.35,0.42)	0.03 (0.01,0.08)	0.14 (0.09,0.2)	0.44 (0.39,0.5)
Age at Exposure & Year of CT	1	6083	1 (1,1)	–	–	–
Age at Exposure & Year of CT	2	2081	0.57 (0.54,0.6)	0.43 (0.41,0.46)	–	–
Age at Exposure & Year of CT	3	2048	0.52 (0.49,0.56)	0.15 (0.11,0.2)	0.33 (0.29,0.37)	–
Age at Exposure & Year of CT	4	2106	0.48 (0.44,0.53)	0.11 (0.07,0.16)	0 (0,1)	0.41 (0.38,0.44)

Table 2
Mean, median, and upper 99th percentile of interval times (years) of CT scans in each latent class. In the chosen model (3 classes and two covariates) the mean interval time for the first and second classes were similar (0.03 years vs. 0.2 years). In all models with more than one class, the last class is markedly different from all the other classes.

	Class 1			Class 2			Class 3			Class 4		
Total Classes	mean	Median	99th%	mean	Median	99th%	mean	Median	99th%	mean	Median	99th%
1	3.00	2.08	13.81	–	–	–	–	–	–	–	–	–
2	0.05	0.03	0.22	6.99	4.85	32.21	–	–	–	–	–	–
3	0.03	0.02	0.15	0.20	0.14	0.91	9.68	6.71	44.60	–	–	–
4	0.04	0.03	0.20	0.09	0.06	0.40	0.45	0.31	2.07	7.43	5.15	34.23

respectively.

3.3. Posterior probability classifiers

The crossover classification method found that interval time cut offs were as follows: younger-early group: 8.7 months; younger-late group: 5.8; months; older-early group: 4.8 months; and older-late group: 3.3 months. This method indicates an exclusion period greater than or equal to 8.7 months is appropriate.

The 99th percentile classification method found that interval time cut offs were as follows: younger-early group: 18.9 months; younger-late group: 15.0; months; older-early group: 8.1 months; and older-late group: 6.8 months. This method indicates an exclusion period greater than or equal to 18.9 months is appropriate.

Fig. 2 demonstrates the relationship between posterior probabilities and interval times. The lines cross at the time when the probability of being in the later class becomes greater than that of being in the earlier class. While the crossover occurs around six months, the probability of being in the potentially causal class does not reach 99% for several months after the crossover and is different depending on age group and year of CT scan.

A sensitivity analysis demonstrated stability for exclusion periods less than or equal to 2 years, with even the simplest model suggesting an exclusion period of less than 2 years. A 3-class model without covariates, or including only CT scans of the brain suggested an overall exclusion period of 19.5 months. In addition, we excluded all persons diagnosed with a cancer after the age of 19, and a tested a 3 class model without covariates which suggested an overall exclusion period of 22.9 months.

3.4. Clinical perspective: percentiles of the PSI

In a separate complementary analysis of the time interval between first symptoms and diagnosis we searched a total of 1,906 abstracts; 20 articles met the inclusion criteria. Table 3 lists the 20 studies reporting PSIs for children diagnosed with brain cancers, with a total of 3,223

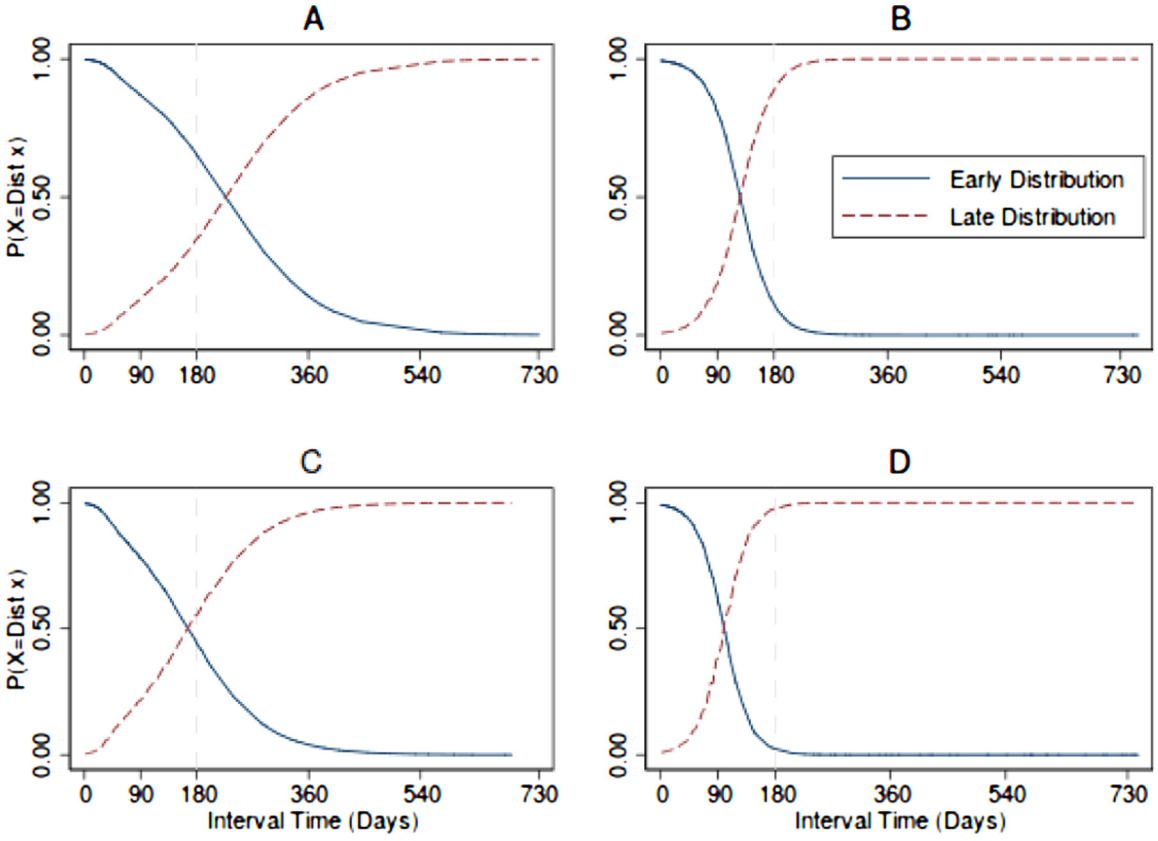

Fig. 2. Posterior Probabilities. A = Young (< 12 years) and Early Period (< 1993), B = Older and Early Period, C = Young and Late Period, D = Older and Late Period. The lines represent the probability of belonging to a particular class at a particular interval period. The posterior probability of being in the first two classes (reverse causation class) decreases to less than 1 percent at 19 months (young group before 1993). This cutoff is as short as 6.8 months in the older group after 1993. The dashed line is at 6 months. The crossover represents the time point when there is an equal probability of being in both classes.

Table 3
Results of the literature review.

Author	Year	n	Age	Histology/Location	Country	PSI	Reported mean (weeks)	Reported median (weeks)	Reported upper limit (weeks)	P_{95} (months)
Dorner et al. [27]	2007	50	Mean 8.1 years	Astrocytoma 30%, medulloblastoma 30%, ependymoma 12%	Germany	Mean 20.3 weeks	20.2		76.4	15.2
Reulecke et al. [28]	2008	245	Mean 6.83 years, (range 0–19.2)	Low-/high-grade gliomas, medulloblastomas, ependymomas, germ cell tumors, meningiomas	Germany	Median 3.4 weeks (0–114 weeks)	8.5	3.4	113.6	3.7
Kukal et al. [29]	2009	315	Median 6.7 years	Infratentorial, supratentorial, and supratentorial midline	Switzerland	Mean 8.6 weeks	8.6		497.1	6.4
Hayashi et al. [30]	2010	60	Median 5.8 years	Embryonal tumors 22%, astrocytoma 18%	Japan	Median 3 weeks		3	142.9	3.2
Shay et al. [31]	2011	330	Mean 8 years (SD 4.9; range 0–18 years)	Most tumors (61%) were gliomas and 15.7% were found to be primitive neuroectodermal tumors, including medulloblastomas. Sixty-six percent of all tumors were low-grade tumors. Only 48% of all tumors were infra-tentorial.	Israel	Mean 7.7 months (range 0.01–108)	30.8		432	23.1
Cecen et al. [32]	2011	82	< 20 years	CNS tumors	Turkey	Median 8.1 weeks (range 1–360)		8.1	360	8.8
Brasme et al. [16]	2012	166	Median 6 years (IQR 5)	Medulloblastomas only	France	Median 9.3 weeks (IQR 2.9–15.7; range 0.4–65.3)	14.3	9.3	65.3	10
Wilne et al. [33]	2012	139	Median 8.1 years (range 29 days to 16.7 years)	Pilocytic Astrocytoma 27%, medulloblastoma 22%	United Kingdom	Median 3.3 months (range 0–6.9 years)		13.1	359.8	14.2
Gerber et al. [34]	2012	224	Median, 7.5 years (range 2.9–17.5)	Medulloblastomas only	Switzerland and Germany	Median 2.0 months (IQR 0–4; range 0.1–48.0)		8	192	8.6
Phi et al. [35]	2012	181	Median 13.0 years (range 1 month to 44 years), 25 patients (13.8%) older than 20 years	Intracranial germ cell tumors	South Korea	Median 2 months (range 0–86)		8	344	8.6
Hamdane et al. [36]	2012	63	< 16 years (range 8 months to 16 years)	None reported	Tunisia	Median 9 weeks (range 0–416)	49	9	416	9.7
Molineus et al. [37]	2013	79	Mean 9.2 years (range 0.2–23.5)	Low-grade gliomas (39%), medulloblastomas (20%), ependymomas (13%), high-grade gliomas (8%) and craniopharyngiomas (8%), cavernomas (3%), germ cell tumors (3%)	Germany	Median 13.6 weeks		13.6		14.7
Kameda-Smith et al. [17]	2013	66	Mean 7.50 years (SD 4.53)	Posterior fossa tumors, pilocytic Astrocytoma 35%, medulloblastoma 35%, ependymoma 10%	Scotland	Median 6.2 weeks	17.3	6.2	40.3	6.7
Veneroni et al. [38]	2013	121	Median 10 (IQR 11)	Not reported	Italy	Median 6.7 days (IQR 1.1–12.3)		6.7	14.4	7.3
Araz et al. [39]	2013	65	Children	CNS tumors	Turkey	Median 7.4 weeks (IQR 8.6–17.1 weeks**)		7.4		8.0
Sethi et al. [20]	2013	70	Median 11.7 years (range 6.2–21.7)	Intracranial germ cell tumors	United States of America	Median 6 months (range 0–72)		24	288	25.9
Maaty et al. [40]	2013	456	Median 8.2 years (range < 1–16)	Most common tumors were low-grade glioma (27.5%), medulloblastomas (25.7%), high-grade gliomas (15.3%), and craniopharyngiomas (8.7%)	Egypt	Median 8.6 weeks		8.6		9.3
Fukuoka et al. [41]	2014	127	Median 7.2 years	Low-grade gliomas 28%, germ cell tumors 22%, medulloblastomas 10%, high-grade gliomas 4%	Japan	Median 1.5 months	20	6	144	6.5
Ramaswamy et al. [42]	2014	126	Median 7.35 years (IQR 4.8)	Medulloblastomas only	Canada	Median 4 weeks (IQR 0–12)		4		4.3
Arnautovic et al. [43]	2015	258	Median 7.1 years (range 0.1–20.7)	Low-grade gliomas	United States of America	Median 2.1 months (range, 0–131.1)		8.3	524.4	3670.8

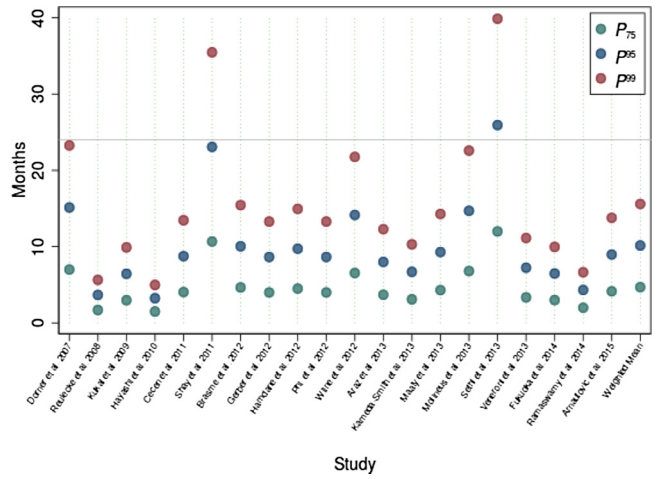

Fig. 3. Results of the literature review and the key result. The sample-size weighted mean of the 99th percentile of the PSI (P_{99}) was 15.6 months. The horizontal line represents 2 years.

children included. All studies reported a mean or median age less than 20, and of those with reported age ranges, almost all reported the upper range of age as less than 25 years. One included study had a median age of 13 and an upper range of 44 years. All studies included children less than 20 years of age (all measures of centrality below ten years of age). Studies came from Europe (9), North America (3), Japan and South Korea (3), Africa (2), Turkey (2), and Israel (1).

The median PSI reported from our literature review was 8.2 weeks (IQR 4.8), or approximately two months. The sample-size weighted means of the P75, P95, and P99 were 4.7, 10.1, and 15.6 months, respectively.

Fig. 3 illustrates the estimated P_{75}, P_{95}, and P_{99} based on the median (or mean in three studies). The reported studies often pooled low- and high-grade tumors. Of the five studies with a P95 greater than one year, four studies had a high proportion of slow-growing tumors. Shay et al. 2011 included 66% low-grade tumors. Twenty-seven percent of the tumors included by Wilne et al. 2012 were pilocytic astrocytomas. Molineus et al. 2013 included 39% low-grade gliomas. Sethi et al. 2013 included only intracranial germ-cell tumors (known to have the longest PSI). [20]

4. Discussion

Using an FMM, we found three latent classes, two of which were deemed to represent the reverse causation class, and the other a potentially causal class. The model suggests that CT scans occurring more than one or two yearsbefore diagnosisbelong to a unique class, termed here the "potentially causal" class of CT scans.

Overall, results from the data-driven FMM model were consistent with clinical data (PSI data). The upper 99th percentile of the interval time for the first latent class was approximately 18.9 months (reverse causation class). Thus, 99% of CT scans belonging to the reverse causation class will have occurred within 18.9 months of diagnosis. Using the crossover classification method, a cutoff of 8.7 months would inform the choice of exclusion periods. In the clinical dataset, the 99th percentile of the PSI was 16 months, implying that a CT scan occurring at least 16 months before the diagnosis of brain cancer is unlikely to have been prompted by symptoms of underlying brain cancer.

The FMM 99th percentile classifier fits better with the 99th percentile of the PSI and thus we believe the that the application of an exclusion period of two years may be better than one year as suggested by the crossover classifier and sensitivity analyses.

This review was not performed to update the literature but rather to create a dataset of clinical information to assess the validity of the FFM model. Other systematic reviews have obtained similar results to ours, reinforcing the notion that CT scans occurring more than two years from diagnosis are unlikely to represent reverse causation scans. Brasme et al. 2012 found the median time to diagnosis for all brain cancers and for high-grade gliomas alone to be seven weeks [21]. Using the methods outlined above, the P_{99} would be 47 weeks, or 11.6 months. Medulloblastomas had a median PSI of 7.9, which equates to a P_{99} of 52 weeks, or 13 months [21]. Benign or low-grade astrocytomas had a median PSI of 19.5 weeks, equivalent to a $P_{99}$of 130 weeks, or 32 months [21]. Both the Brasme et al. 2012 and the review by Wilne et al. 2007 found that slow-growing tumors had longer PSIs [15, 21]. Thus, these findings are consistent with those from the mixture model, which show that CT scans performed more than two years prior to the diagnosis of cancer are unlikely to represent scans performed due to of symptoms of underlying brain cancer. In fact, these studies suggest exclusion periods as short as one year.

4.1. Strengths and limitations

The key strength of this study is that the Medicare dataset is truly population-based. The Medicare dataset was linked to a cancer outcome registry noted to be grade “A” according to the International Agency for Research on Cancer (IARC)’s “Cancer incidence in five continents” [22]. In addition, we used clinical data to inform our choice of classifier.

This study is limited because we did not capture CT scans occurring in persons after the age of 20. Thus, persons diagnosed with a brain tumor after the age of 20 would only be in the potentially causal class because their interval times will as long as their age at diagnosis minus 19. Another limitation is that 274 brain cancers were diagnosed after the age of 19, which is slightly different to the narrative review that included only persons diagnosed below the age of 20 years of age.

Another limitation is that we did not capture all CT scans occurring in state-funded hospitals where radiology services were not funded by the federal government through Medicare (Several public hospitals operate a public-private model, where CT scans are billed to Medicare). Thus, some CT scans occurring in children presenting to the emergency department of a state hospital (i.e. after a seizure or signs of severe raised intracranial pressure) would not be captured in the Medicare records..

Exclusion periods are not intended to manage bias arising from the latency period [23,24] which is the period between disease initiation and start of the PSI. Exposures in the latency phase of cancer could be potentially causal through the growth promotional effects of radiation [25,26]. However, the focus of this study was to use exclusion periods (or exposure lagging) to manage reverse causation bias in epidemiological studies, and *not* to assess latency bias.

Overall, this analysis is robust because we used a large database with a data-driven approach that is backed by clinical information. The dataset (> 1000 persons with a CT scan and a brain cancer diagnosis) is one of the largest collections of CT scan exposures and cancer diagnoses, allowing for stable and accurate estimates. Although a number of exposures and outcomes could have been missed, we do not believe that this has invalidated our major conclusions.

5. Conclusions

Our finite mixture modelling suggests that an exclusion period of one to two years following CT scan radiation will exclude almost all cases of brain cancer attributable to reverse causation. This conclusion is supported by an analysis of clinical studies reporting the intervals of time between first symptoms and diagnoses of brain cancer.This information will be useful to epidemiologists defining exclusion periods or lag periods for use in future cohort studies.

Ethical approval

This study was approved by the Human Research Ethics Committee of the University of Melbourne and by ethics committees, data custodians, and cancer registrars of the Australian Government Department of Health, Medicare, the Australian Institute of Health and Welfare, and all states and territories of Australia.

Author contributions

NRS conceived the clinical study, analyzed the data, and drafted the manuscript. JDM provided supervision, access to linked data, and suggested the use of mixture modeling. KS provided statistical oversight. All authors edited the manuscript and approved the final version.

Funding

This work was funded by the Australian Government through NHMRC grants 509190, 1027368, and 1084197.

Acknowledgments

We thank colleagues who contributed to our earlier publication and colleagues from the University of Melbourne and the Australian Institute of Health and Welfare, who provided advice and data for this new work.

References

[1] D.J. Brenner, R. Doll, D.T. Goodhead, et al., Cancer risks attributable to low doses of ionizing radiation: assessing what we really know, Proc. Natl. Acad. Sci. U S A 100 (24) (2003) 13761–13766, https://doi.org/10.1073/pnas.2235592100.
[2] Committee to Assess Health Risks from Exposure to Low Levels of Ionizing Radiation, Health Risks from Exposure to Low Levels of Ionizing Radiation: BEIR VII-Phase 2, 7th ed., The National Academies Press, Washington DC, 2006http://cds.cern.ch/record/1016006.
[3] D.B. Richardson, E. Cardis, R.D. Daniels, et al., Risk of cancer from occupational exposure to ionising radiation: retrospective cohort study of workers in France, the United Kingdom, and the United States (INWORKS), BMJ 351 (2015) h5359, https://doi.org/10.1136/bmj.h5359.
[4] M. Tubiana, L.E. Feinendegen, C. Yang, J.M. Kaminski, Linear no-threshold relationship is inconsistent with radiation biologic and experimental data, Radiology 251 (1) (2009) 13–22, https://doi.org/10.1148/radiol.2511080671.
[5] J.A. Siegel, C.W. Pennington, B. Sacks, Subjecting radiologic imaging to the linear no-threshold hypothesis: a non sequitur of non-trivial proportion, J. Nucl. Med. 58 (1) (2017) 1–6, https://doi.org/10.2967/jnumed.116.180182.
[6] M.Z. Braganza, C.M. Kitahara, A. Berrington de González, P.D. Inskip, K.J. Johnson, P. Rajaraman, Ionizing radiation and the risk of brain and central nervous system tumors: a systematic review, Neuro Oncol 14 (11) (2012) 1316–1324, https://doi.org/10.1093/neuonc/nos208.
[7] M.S. Pearce, J. Salotti, M.P. Little, et al., Radiation exposure from CT scans in childhood and subsequent risk of leukaemia and brain tumours: a retrospective cohort study, Lancet 380 (9840) (2012) 499–505, https://doi.org/10.1016/S0140-6736(12)60815-0.
[8] J.D. Mathews, A.V. Forsythe, Z. Brady, et al., Cancer risk in 680 000 people exposed to computed tomography scans in childhood or adolescence: data linkage study of 11 million Australians, Br. Med. J. 346 (may21 1) (2013), https://doi.org/10.1136/bmj.f2360 f2360-f2360.
[9] N. Smoll, Z. Brady, K. Scurrah, J. Mathews, Exposure to ionizing radiation and brain cancer incidence: the Life Span Study cohort, Cancer Epidemiol. 42 (2016) 60–65 http://www.ncbi.nlm.nih.gov/pubmed/27038588.
[10] D.L. Preston, E. Ron, S. Yonehara, et al., Tumors of the nervous system and pituitary gland associated with atomic bomb radiation exposure, J. Natl. Cancer Inst. 94 (20) (2002) 1555–1563, https://doi.org/10.1093/jnci/94.20.1555.
[11] L. Walsh, R. Shore, A. Auvinen, T. Jung, R. Wakeford, Risks from CT scans-what do recent studies tell us? J. Radiol. Prot. 34 (1) (2014) E1–5, https://doi.org/10.1088/0952-4746/34/1/E1.
[12] Health Data Standards Committee, Data Set Specification, Cancer (Clinical), National Health Data Dictionary Version 12, Supplement. AIHW Cat. No. HWI 71, (2004).
[13] K.L. Nylund, T. Asparouhov, B.O. Muthén, Deciding on the number of classes in latent class analysis and growth mixture modeling: a Monte Carlo simulation study, Struct. Equ. Model. 14 (4) (2007) 535–569, https://doi.org/10.1080/10705510701575396.
[14] J. Petersen, K. Bandeen-Roche, E. Budtz-Jørgensen, K. Groes Larsen, Predicting latent class scores for subsequent analysis, Psychometrika 77 (2) (2012) 244–262, https://doi.org/10.1007/s11336-012-9248-6.
[15] S. Wilne, J. Collier, C. Kennedy, K. Koller, R. Grundy, D. Walker, Presentation of childhood CNS tumours: a systematic review and meta-analysis, Lancet Oncol. 8 (8) (2007) 685–695, https://doi.org/10.1016/S1470-2045(07)70207-3.
[16] J.-F.-F. Brasme, M. Chalumeau, F. Doz, et al., Interval between onset of symptoms and diagnosis of medulloblastoma in children: distribution and determinants in a population-based study, Eur. J. Pediatr. 171 (1) (2012) 25–32, https://doi.org/10.1007/s00431-011-1480-z.
[17] M.M. Kameda-Smith, J. White M a, E.J. St George, J.I.M. Brown, Time to diagnosis of paediatric posterior fossa tumours: an 11-year West of Scotland experience 2000-2011, Br. J. Neurosurg. 27 (3) (2013) 364–369, https://doi.org/10.3109/02688697.2012.741731.
[18] A. Rohatgi, WebPlotDigitizer, (2017) http://arohatgi.info/WebPlotDigitizer.
[19] M.J. Van Den Bent, T.J. Snijders, J.E.C. Bromberg, Current treatment of low grade gliomas, Memo Mag. Eur. Med. Oncol 5 (3) (2012) 223–227, https://doi.org/10.1007/s12254-012-0014-3.
[20] R.V. Sethi, R. Marino, A. Niemierko, N.J. Tarbell, T.I. Yock, S.M. MacDonald, Delayed diagnosis in children with intracranial germ cell tumors, J. Pediatr. 163 (5) (2013) 1448–1453, https://doi.org/10.1016/j.jpeds.2013.06.024.
[21] J.F. Brasme, M. Morfouace, J. Grill, et al., Delays in diagnosis of paediatric cancers: a systematic review and comparison with expert testimony in lawsuits, Lancet Oncol. 13 (10) (2012) e445–e459, https://doi.org/10.1016/S1470-2045(12)70361-3.
[22] F. Bray, D.H. Brewster, C.G. Mbalawa, B. Kohler, R. Swaminathan, J. Ferlay, Cancer Incidence in Five Continents Vol. X. Vol X, (2020).
[23] K.J. Rothman, Induction periods and latent periods, Am. J. Epidemiol. 114 (2) (1981) 1–12, https://doi.org/10.1093/acprof.
[24] D.B. Richardson, S.R. Cole, H. Chu, B. Langholz, Lagging exposure information in cumulative exposure-response analyses, Am. J. Epidemiol. 174 (12) (2011) 1416–1422, https://doi.org/10.1093/aje/kwr260.
[25] C. Moncharmont, A. Levy, J.B. Guy, et al., Radiation-enhanced cell migration/invasion process: a review, Crit. Rev. Oncol. Hematol. 92 (2) (2014) 133–142, https://doi.org/10.1016/j.critrevonc.2014.05.006.
[26] V.N. Ivanov, T.K. Hei, Radiation-induced glioblastoma signaling cascade regulates viability, apoptosis and differentiation of neural stem cells (NSC), Apoptosis 19 (12) (2014) 1736–1754, https://doi.org/10.1007/s10495-014-1040-x.
[27] L. Dörner, M.J. Fritsch, A.M. Stark, H.M. Mehdorn, Posterior fossa tumors in children: how long does it take to establish the diagnosis? Childs Nerv. Syst. 23 (2007) 887–890, https://doi.org/10.1007/s00381-007-0323-8.
[28] B.C. Reulecke, C.G. Erker, B.J. Fiedler, T.-U.-U. Niederstadt, G. Kurlemann, Brain tumors in children: initial symptoms and their influence on the time span between symptom onset and diagnosis, J. Child Neurol. 23 (2) (2008) 178–183, https://doi.org/10.1177/0883073807308692.
[29] K. Kukal, M. Dobrovoljac, E. Boltshauser, R. Ammann, M. Grotzer, Does diagnostic delay result in decreased survival in paediatric brain tumours? Eur. J. Pediatr. 168 (2009) 303–310, https://doi.org/10.1007/s00431-008-0755-5.
[30] N. Hayashi, H. Kidokoro, Y. Miyajima, et al., How do the clinical features of brain tumours in childhood progress before diagnosis? Brain Dev. 32 (8) (2010) 636–641, https://doi.org/10.1016/j.braindev.2009.10.001.
[31] V. Shay, A. Fattal-Valevski, L. Beni-Adani, S. Constantini, Diagnostic delay of pediatric brain tumors in Israel: a retrospective risk factor analysis, Childs Nerv. Syst. 28 (1) (2012) 93–100, https://doi.org/10.1007/s00381-011-1564-0.
[32] E. Cecen, D. Gunes, K. Mutafoglu, F. Sarialioglu, N. Olgun, The time to diagnosis in childhood lymphomas and other solid tumors, Pediatr. Blood Cancer 57 (3) (2011) 392–397, https://doi.org/10.1002/pbc.23072.
[33] S. Wilne, J. Collier, C. Kennedy, et al., Progression from first symptom to diagnosis in childhood brain tumours, Eur. J. Pediatr. 171 (1) (2012) 87–93, https://doi.org/10.1007/s00431-011-1485-7.
[34] N.U. Gerber, K. Von Hoff, A.O. Von Bueren, et al., A long duration of the pre-diagnostic symptomatic interval is not associated with an unfavourable prognosis in childhood medulloblastoma, Eur. J. Cancer 48 (13) (2012) 2028–2036, https://doi.org/10.1016/j.ejca.2011.11.012.
[35] J.H. Phi, S.K. Kim, Y.A. Lee, et al., Latency of intracranial germ cell tumors and diagnosis delay, Childs Nerv. Syst. 29 (10) (2013) 1871–1881, https://doi.org/10.1007/s00381-013-2164-y.
[36] M.M. Hamdane, F. Bougrine, M. Ben Ammar, I. Msekni, M. Yedes, A. Bouziani, Le retard diagnostique dans les tumeurs du système nerveux central de l'enfant, J Africain du Cancer / African J Cancer 4 (4) (2012) 228–232, https://doi.org/10.1007/s12558-012-0229-6.
[37] A. Molineus, N. Boxberger, A. Redlich, P. Vorwerk, Time to diagnosis of brain tumors in children: a single-centre experience, Pediatr. Int. 55 (3) (2013) 305–309, https://doi.org/10.1111/ped.12095.
[38] L. Veneroni, L. Mariani, S. Lo Vullo, et al., Symptom interval in pediatric patients with solid tumors: adolescents are at greater risk of late diagnosis, Pediatr. Blood Cancer 60 (4) (2013) 605–610, https://doi.org/10.1002/pbc.24312.
[39] N.C. Araz, E. Guler, Delays in diagnosis of childhood cancer in southeastern Turkey and the associated factors, Pediatr. Hematol. Oncol. 32 (2) (2015) 153–163, https://doi.org/10.3109/08880018.2013.874511.
[40] H.I. Maaty, A long-term evaluation of latency of pediatric brain tumors diagnosis in province of Delta-Egypt, J. Neurol. Sci. 333 (2013) e655–e656, https://doi.org/10.1016/j.jns.2013.07.2272.
[41] K. Fukuoka, T. Yanagisawa, T. Suzuki, et al., Duration between onset and diagnosis in CNS tumors: impact on prognosis and functional outcome, Pediatr. Int. (April) (2014) 829–833, https://doi.org/10.1111/ped.12369.
[42] V. Ramaswamy, M. Remke, D. Shih, et al., Duration of the pre-diagnostic interval in medulloblastoma is subgroup dependent, Pediatr. Blood Cancer 61 (7) (2014) 1190–1194, https://doi.org/10.1002/pbc.25002.
[43] A. Arnautovic, C. Billups, A. Broniscer, A. Gajjar, F. Boop, I. Qaddoumi, Delayed diagnosis of childhood low-grade glioma: causes, consequences, and potential solutions, Childs Nerv. Syst. (2015) 1067–1077, https://doi.org/10.1007/s00381-015-2670-1.